

Nucleation Control for Large, Single Crystalline Domains of Monolayer Hexagonal Boron Nitride via Si-Doped Fe Catalysts

*Sabina Caneva¹, Robert S. Weatherup¹, Bernhard C. Bayer^{1,2}, Barry Brennan³, Steve J. Spencer³, Ken Mingard³, Andrea Cabrero-Vilatela¹, Carsten Baehtz⁴, Andrew J. Pollard³ and Stephan Hofmann¹. **

¹Department of Engineering, University of Cambridge, JJ Thomson Avenue, CB3 0FA, Cambridge, UK.

²Faculty of Physics, University of Vienna, Boltzmanngasse 5, A-1090 Vienna, Austria

³National Physical Laboratory, Hampton Rd, TW11 0LW, Teddington, Middlesex, UK.

⁴Institute of Ion Beam Physics and Materials Research, Helmholtz-Zentrum Dresden-Rossendorf, 01314 Dresden, Germany.

*Corresponding Author: sh315@cam.ac.uk

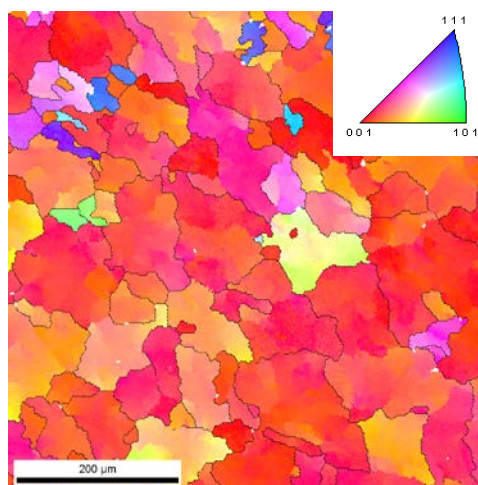


Figure S1. Electron backscatter diffraction (EBSD) map of the post-growth surface of a Fe(1000 nm)/SiO₂(300 nm)/Si substrate after air exposure. The map was acquired with a step size of 2.5 μm and shows the orientation of the α -Fe bcc phase using an inverse pole figure color key in the substrate normal direction (inset); grain boundaries with misorientations $> 15^\circ$ shown in black. For this sample the variation in color within each grain shows the presence of sub-grain boundaries $< 15^\circ$ while the dominance of pink/red colors indicates a strong $<001>$ texture

normal to the substrate with random in-plane rotation about the normal. The mean circle equivalent diameter grain size is $47\text{ }\mu\text{m}$.

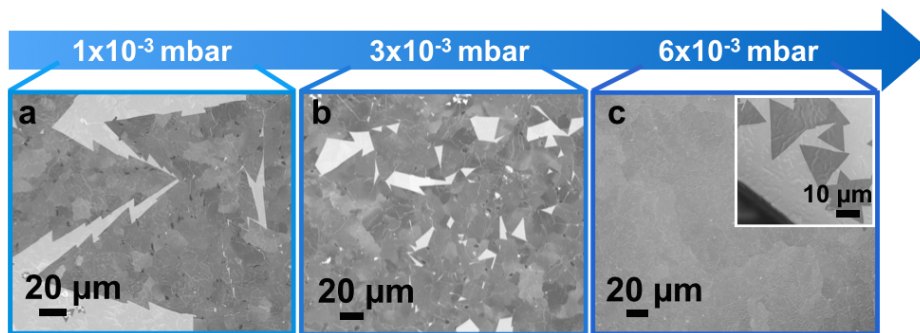


Figure S2. (a) Low pressure growth ($1 \times 10^{-3} \text{ mbar}$) showing h-BN domains at the onset of coalescence. (b) Medium pressure growth ($3 \times 10^{-3} \text{ mbar}$) showing an increase in the nucleation density and a slight decrease in domain size. (c) High pressure growth ($6 \times 10^{-3} \text{ mbar}$) showing a continuous h-BN film homogeneously covering the Fe surface. The inset shows the nucleation stage for this film and displays domains with lateral sizes of $> 25\text{ }\mu\text{m}$. All growths were performed at $940\text{ }^{\circ}\text{C}$ for 5 min.

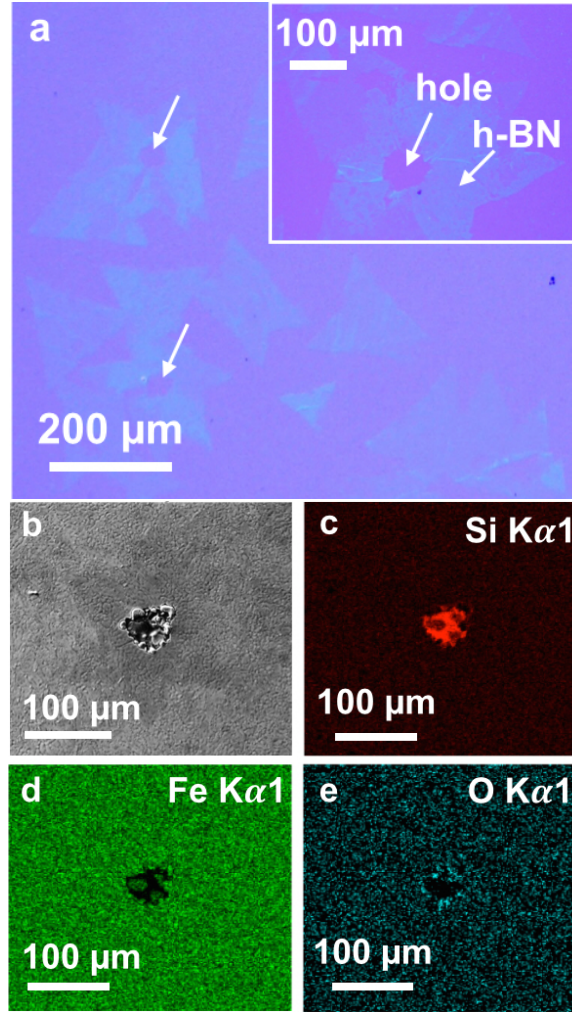


Figure S3. (a) Optical image of transferred h-BN showing holes corresponding to the location of the craters. (b) SEM image of the post-growth surface of a Fe/SiO₂(200 nm)/Si sample showing a surface crater surrounded by h-BN domains. The growth was performed at 940 °C and 1×10^{-3} mbar borazine pressure for 5 min. (c), (d), (e) SEM-EDX chemical maps of Si, Fe and O distribution respectively on the crater in (b). We note that the detection limit of the technique is 0.1-1 at%.

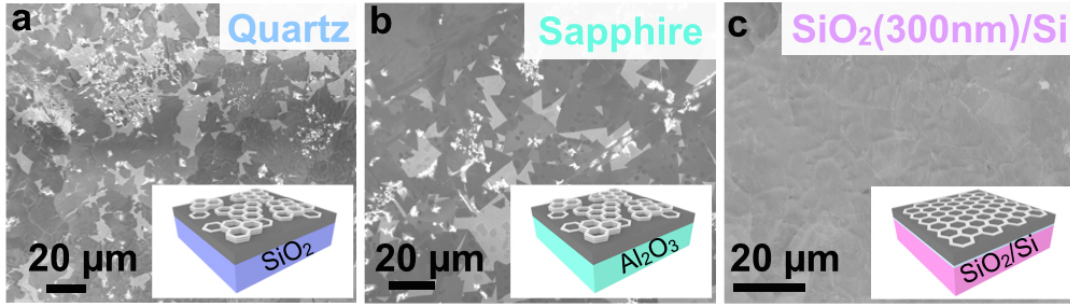


Figure S4. Comparison of h-BN grown on alternative substrates at 940 °C and 6×10^{-3} mbar for 5 min on (a) Fe(1000 nm)/quartz. (b) Fe(1000 nm)/sapphire. (c) Fe(1000 nm)/SiO₂(300 nm)/Si.

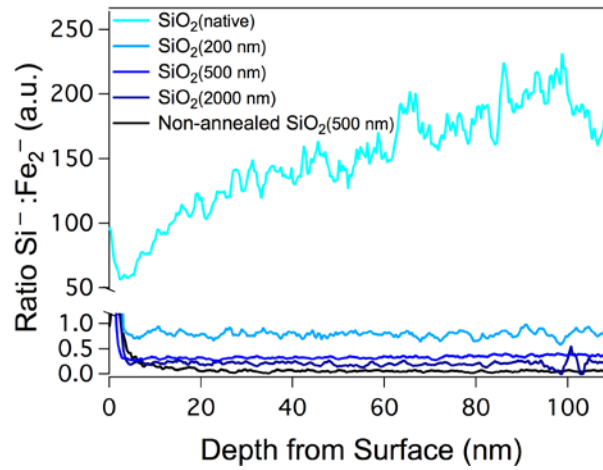


Figure S5. Plot of Si⁻:Fe₂⁻ ratio as a function of depth from the surface for samples with native, 200 nm, 500 nm, 2000 nm and the reference non-annealed 500 nm oxide. All samples were grown at 3×10^{-3} mbar, 940 °C for 5 min. We note that although the concentrations of Si in the post-growth samples with SiO₂(200 nm), SiO₂(500 nm) and SiO₂(2000 nm) are distinctly different (Figure 3 f,i,l), the Si⁻:Fe₂⁻ ratios do not significantly change with sample depth for the analyzed region.

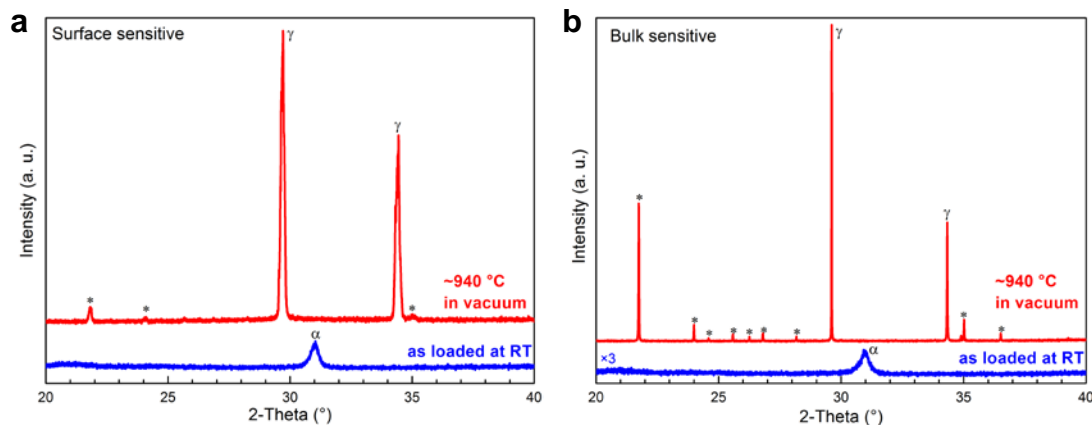


Figure S6. Comparison of (a) surface-sensitive (data replotted from Figure S5) and (b) bulk-sensitive *in-situ* XRD patterns of a Fe(500nm)/SiO₂(300nm)/Si sample (bottom: as loaded, top: during vacuum annealing at 940 °C) showing the appearance of iron silicate (Fe₂SiO₄ reflections labelled with “*”) during annealing *prior* to borazine exposure. We note that the assignment of the “*” to Fe₂SiO₄ is based on reasonable agreement in observed diffraction angles compared to powder database entries, but that the reflection intensity ratios are different to powder, indicating possibly strong texturing. We emphasize however that the silicate assignment is also corroborated by the absence of “*” reflections for Fe films on Si-free sapphire supports upon the same processing (see Figure S9). The Fe undergoes a thermally induced phase transformation^{1,2} from as deposited α -Fe to γ -Fe (labelled “ α ” and “ γ ”, respectively) upon annealing. The comparison of surface and bulk sensitive XRD patterns illustrates that the silicate is located near the SiO₂-Fe interface, as the relative contribution of the silicate signal compared to the γ -Fe signal is much stronger in the bulk-sensitive scan. (Note that the signal intensity for the as loaded scan was multiplied by a factor of 3 to enhance the readability of the figure).

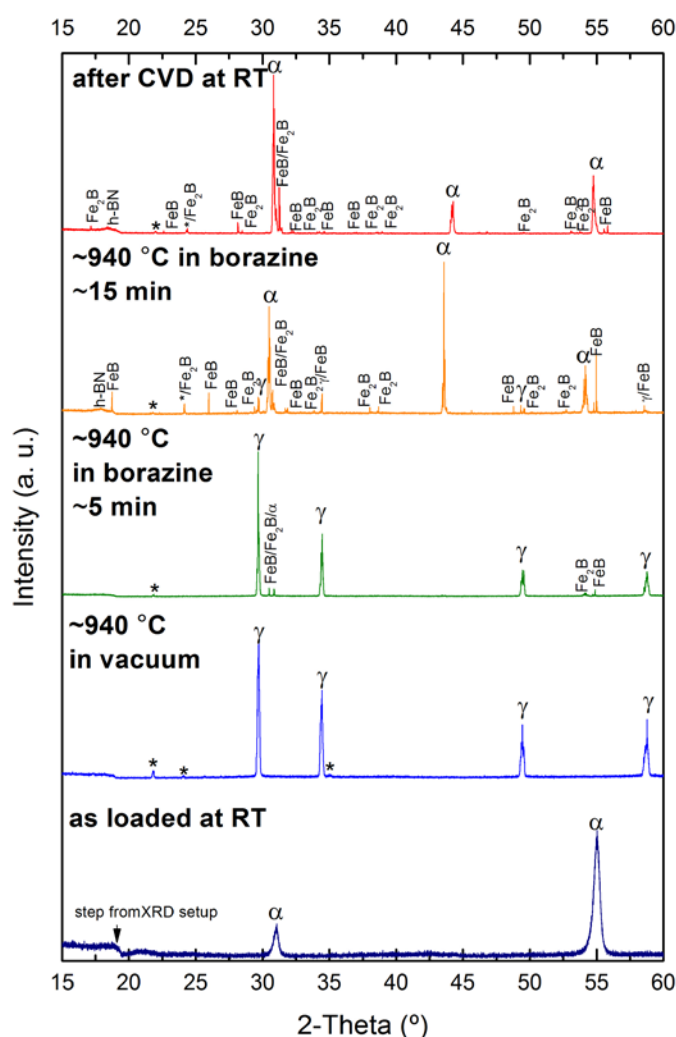


Figure S7. Same surface sensitive *in-situ* XRD patterns of a Fe(500 nm)/SiO₂(300 nm)/Si sample during the salient stages of the CVD process as plotted in Figure 4(a) but with diffracted intensity plotted on a linear scale (in contrast, Figure 4(a) is plotted with intensity on log scale to emphasize the presence of minority phases). The comparison of the intensity scaling clearly shows that, while Fe-borides are observed for extended borazine exposures, the majority catalyst phase remains metallic Fe throughout the entire CVD process. “α” denotes reflections from α-Fe, “γ” from γ-Fe, “*” from iron silicate Fe₂SiO₄, “FeB” from FeB, “Fe₂B” from Fe₂B and “h-BN” from h-BN, respectively. Comparison to bulk-sensitive XRD scans during the same processing indicates that the Fe-borides are located near the catalyst surface, as stronger Fe-boride signatures are observed in the surface-sensitive scans compared to the bulk-sensitive scans. We also note here that some of the observed reflections in the γ-Fe, FeB and Fe₂B signatures could also be partially assigned to the structural Fe-nitrides ε-Fe_xN (ICSD: 80930) or γ'-Fe₄N (ICSD: 79980). Control experiments with similar Fe films exposed to up to 4 mbar NH₃ at 940 °C however exclude formation of ε-Fe_xN, and the presence of γ'-Fe₄N at 940 °C can be excluded

based on its known stability of only up to 680 °C.¹ Therefore FeB and Fe₂B are assigned with a high degree of confidence.

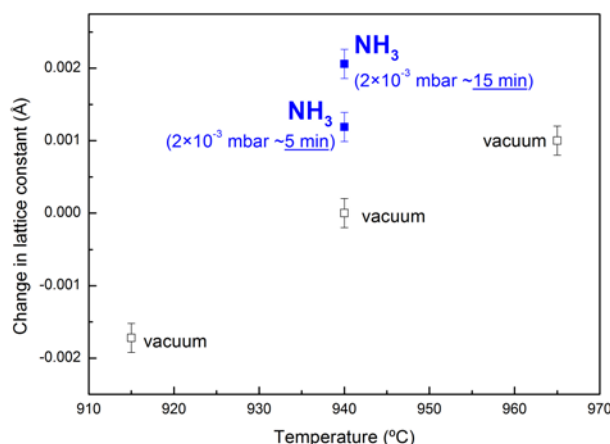


Figure S8. Change in γ -Fe lattice parameter of a Fe(500nm)/SiO₂(300nm)/Si sample during vacuum and NH₃ exposure (2×10^{-3} mbar, 5min and 15 min) at 940 °C (corrected for thermal expansion via measuring a baseline temperature series in vacuum). Quantitative lattice parameters were derived by Rietveld refinement of surface sensitive XRD measurements (using X'Pert Plus and file 44862 from the Inorganic Crystal Structure Database (ICSD)). When NH₃ is introduced the Fe lattice constant expands by ~ 0.001 Å (5 min) and ~ 0.002 Å (15 min), respectively, compared to the vacuum baseline. As NH₃ is known to dissociate on Fe at these conditions,³ this lattice expansion is indicative of interstitial uptake of nitrogen into the γ -Fe lattice. Comparison with thermodynamic reference data suggests that ~ 2.5 atom-% N are interstitially dissolved in the γ -Fe lattice.¹ Refinement of concurrently acquired bulk-sensitive XRD patterns did not show a corresponding increase in the γ -Fe lattice parameter, indicating that the N is predominantly dissolved near the surface of the Fe films for the applied NH₃ pressure and exposure times.

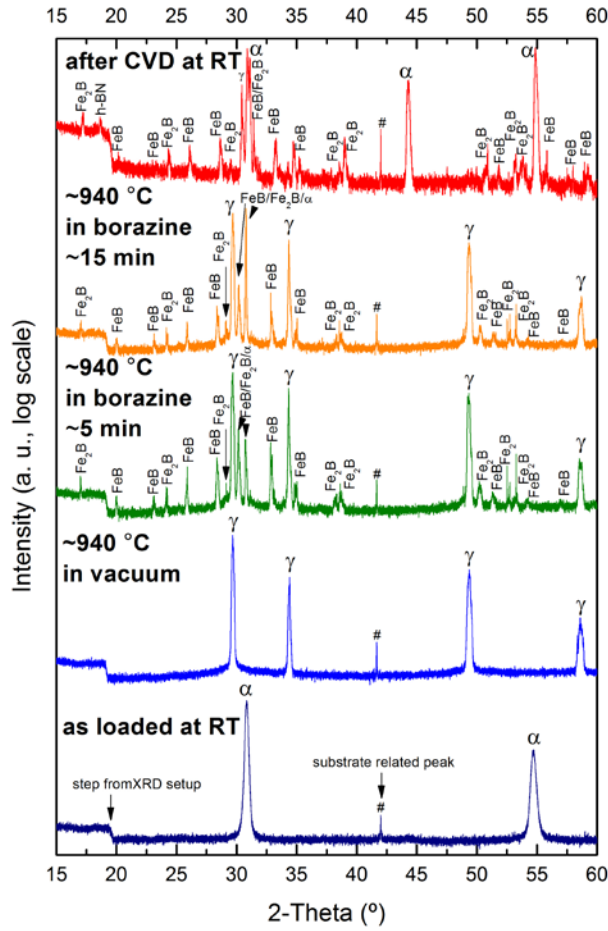


Figure S9. Surface sensitive *in-situ* XRD patterns of a Fe(500 nm)/sapphire sample during the salient stages of the CVD process. We note that diffraction intensity is plotted on a log scale in this figure to enhance the visibility of minority phases. This XRD data on sapphire supported Fe helps to identify the effect of Si diffusion upon phase evolution via comparison to Figure 4(a), where similar *in-situ* XRD scans are plotted for a Fe(500 nm)/SiO₂(300 nm)/Si sample: Similar as on SiO₂(300 nm)/Si, the Fe on sapphire undergoes a thermally induced^{1,2} phase transformation from as deposited α -Fe to γ -Fe (labelled “ α ” and “ γ ”, respectively) upon heating to 940 °C. Importantly, no reflections which have been assigned to iron silicates (Fayalite, Fe₂SiO₄) are observed on the Si-free sapphire sample, further corroborating the silicate assignment for the SiO₂/Si sample. With borazine exposure Fe-boride phases (FeB and Fe₂B) emerge (as for the SiO₂/Si sample, but in contrast already within the first 5 min), however even for extended borazine exposure (15 min) only a small amount of α -Fe is formed at 940 °C (where we suggest that this minor α -Fe formation may be related to B uptake into the Fe catalyst). The lack of a comparably appreciable isothermal γ -Fe to α -Fe transition on the Si-free sapphire sample as in the SiO₂/Si sample (Figure 4(a)) even for extended borazine exposures indicates that this γ -Fe to

α -Fe transformation is otherwise largely related to continued Si diffusion into the Fe. This is also in excellent agreement with the Fe-B-Si phase diagram,⁴ which suggest γ -Fe to α -Fe transitions for increasing Si influx. Upon cooling to room temperature after CVD the majority catalyst phase reverts to α -Fe in the sapphire sample via a simple temperature induced reverse phase transformation.^{1,2}

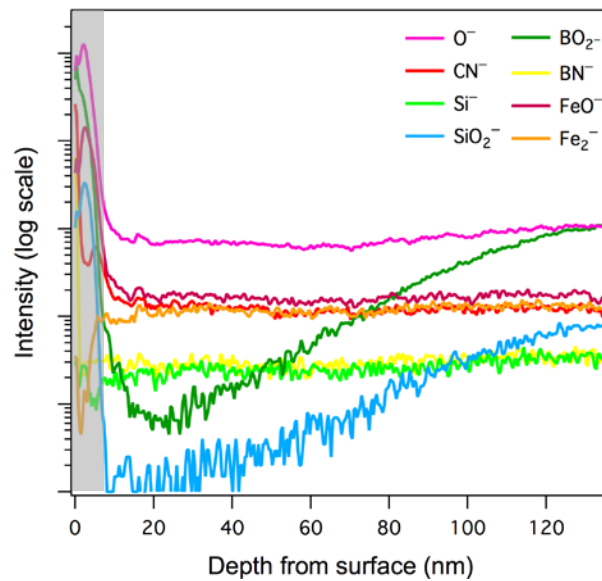


Figure S10. SIMS depth distribution of the top 120 nm from the surface of B, N, Si and Fe related species of a Fe/SiO₂(500 nm)/Si sample, indicating a number of distinct regions of material distribution, showing a nitrogen rich surface layer followed by an oxygen rich region over the next ~6 nm (shaded area). The h-BN was grown for 5 min at 940 °C and 3×10^{-3} mbar. Signals for B, O₂ and FeO₂ negative ions were also acquired (not shown), and although they are present at the surface and subsurface, the signals are gradually reduced within the first 12 nm and show no further increase with depth. After removal of the nitrogen-rich surface layer, oxide species of Si, Fe and B are detected over the next ~6 nm. Oxide species containing molecular oxygen (O₂⁻) are prevalent indicating that the oxide is likely to be in well-defined chemical states and are not just present due to sputter-induced effects. After the oxide region is removed (shaded gray area) we detect an increase in the Fe₂⁻ ion signal and a decrease of the O₂⁻ signal to within the SIMS detection limit. However, there is still clearly oxygen distributed throughout the iron layer, with O⁻, FeO⁻, BO₂⁻ and SiO₂⁻ ion signals still detected. The absence of an O₂⁻ signal indicates that the remaining oxide species are in less well-defined chemical states than in the surface region. The subsequent increase in the SiO₂⁻ and O⁻ signals indicates an increased oxide concentration closer to the Fe/SiO₂ interface.

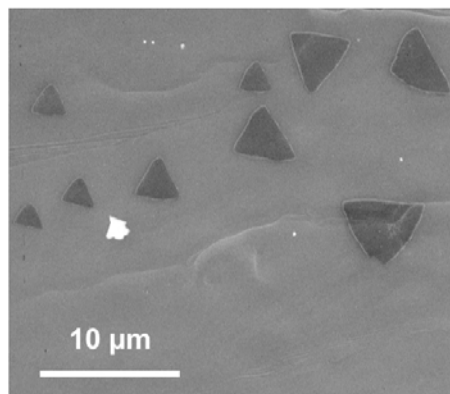


Figure S11. SEM image of h-BN nuclei formed on a Fe/SiO₂(200 nm)/Si substrate. The growth was performed at 940 °C and 3×10^{-3} mbar borazine exposure for < 1 min.

References

- (1) Wriedt, H.; Gokcen, N.; Nafziger, R. *Bull. Alloy Phase Diagr.* **1987**, 8, 355–377.
- (2) Okamoto, H. *J. Phase Equilibria Diffus.* **2004**, 25, 297–298.
- (3) Grunze, M.; Bozso, F.; Ertl, G.; Weiss, M. *Appl. Surf. Sci.* **1978**, 1, 241–265.
- (4) Raghavan, V. *J. Phase Equilibria Diffus.* **2007**, 28, 380–381.